MONITORING OF ROLLER BEARINGS: ELECTRICAL VS VIBRATIONAL ANALYSIS

E. Chevallier[a,*], J. C. Boudimbou[b], R. Bouzerar[c], T. Garcia[d], F. Bolaers[a] and X. Chiementin[a]

*eddy.chevallier@univ-reims.fr

[a] Institut de Thermique, Mécanique, Matériaux, (ITheMM – UR URCA 7548), Université de Reims Champagne-Ardenne, Campus du Moulin de la Housse, 51687 Reims, France

[b] Département de Physique, UFR des Sciences, Université de Picardie Jules Verne, 33 rue Saint Leu, 80039 Amiens, France

[c] Laboratoire de Physique de la Matière Condensée (LPMC – UR UPJV 2081), Université de Picardie Jules Verne, 33 rue Saint Leu, 80039 Amiens, France

[d] Laboratoire « Physique des Systèmes Complexes » (PSC – UR UPJV 4663), Université de Picardie Jules Verne, 33 rue Saint Leu, 80039 Amiens, France

KEYWORDS

Predictive maintenance; Defect signatures; Vibrational analysis; Electrical analysis; Roller bearing.

ABSTRACT

We present in this work a qualitative experimental study aiming to compare two bearing monitoring methods. One is based on an electrical probing and the other one on vibrational measurements. Electrical and vibrational signals were acquired according to rotation speeds and radial loads. The electrical method seems to show a complementary approach opening new ways of monitoring.

1. INTRODUCTION

Bearings are one of the most important and frequently used components in rotating machinery, whether in the industrial or transport fields, and present a large range of various applications. An undetected defect in a bearing can lead to catastrophic economic and human consequences: statistical studies show that bearing defects represent more than 40% of malfunction in rotating machinery [1-4]. To respond to these safety and economic imperatives, there has been substantial amount of research on the monitoring and the diagnosis of bearing in order to provide and to improve new condition monitoring techniques. Many experimental methods and various types of signal analysis have been developed for the detection and the diagnosis of bearing defects, such as vibratory analysis [5-8], acoustic emission (AE) [9, 10], stator current analysis [11, 12], thermal and lubrication analysis [13].

Over the past decade, several studies have clearly established the relevance of an electrical method which probes directly the contact in order to highlight the presence of a defect [14-16] or to provide information on the contact degradation [17]. This method is based on the analysis of the voltage noise across the system which is generated by the contact conditions fluctuation during - rolling or sliding - motion, significant of the quality of the contact [18, 19]. In this case, contact quality refers to an acceptable electromechanical contact condition defined by the specifications of an application.

The monitoring of bearings lies on signal processing techniques in both time and frequency domains that can be used as well to process the electrical signals as the vibrational ones. In order to highlight the contributions of the electrical method, this paper analyzes data from electrical probing and vibrations analysis through their respective spectral and statistical properties.

2. MATERIAL AND METHODS

2.1 Material

The studied roller bearing is a NU206ECP from SKF (fig. 1, Table 1). This bearing consists in thirteen cylindrical steel roller with a diameter of 9 mm and a length of 10 mm, which are held by a cage made of reinforced glass fibre “PA66”. According to the manufacturer the material of each part of the bearing is an AISI 52100 (100C6) steel - 1% carbon and 1.5% chrome. The contacting surfaces of the inner ring and a roller were observed using a SEM (Quanta 200FEG, with a micro-analyzer X INCA Oxford type SDD 80 mm^2) and are respectively shown in figure 2a and 2b. The roughness of those surfaces were estimated by contact profilometry using a “DektakXT Stylus Profiler” from Brucker with a 2µm stylus at 3mg of load. A typical measurement is shown on figure 3. The roughness RMS is computed from a dozen locations for each element and is estimadted to 25 nm (±4 nm) for the roller and 49 nm (±10 nm) for the inner ring (the roughness of the outer ring is assumed to be the same).

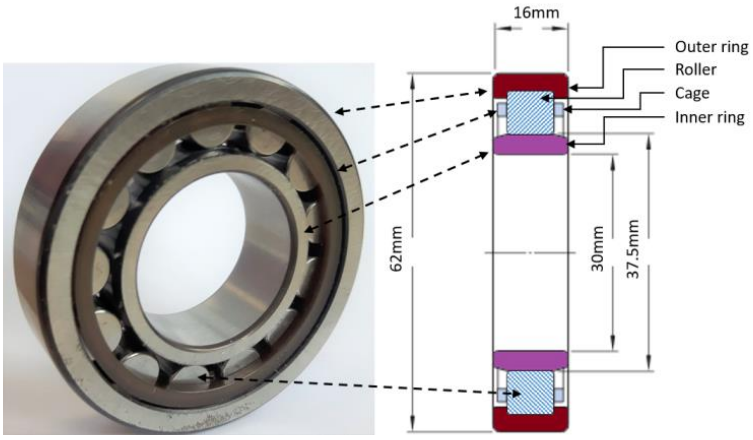

Fig. 1: NU206ECP roller bearing

Symbol	Quantity	Values
D	Outer diameter	62 mm
d	Inner diameter	30 mm
D_m	Pitch diameter	46.5 mm
Z	Number of roller	13
d_{ball}	Roller diameter	9 mm
φ	Angle	0°

Table 1: Characteristics of the NU206 roller bearing

2.2 Apparatus

The apparatus is made of a metallic housing through which a shaft is placed and held by two bearings (in red on fig. 4). Bearings are mounted with a sliding assembly and a nut tightens the inner ring on the shaft. The shaft is connected to a brushless AC servo motor (3000 rpm, 98V, 1.6Nm/A - ref. 190UMB301CACAA). A load is applied at the end of the shaft using a hydraulic cylinder, thus exerting a radial force on bearings (black arrow on fig. 4). Note that the alignment of the shaft has been checked and is less than 0.1 mm.

Electrical measurements are made using a Keithley SourceMeter 2611B. A current flows from the first bearing to the second one via the shaft and the voltage is measured between each end (fig. 5a). Bearings are isolated from the metallic housing using an insulating paint (in yellow on fig. 5a). Wires are connected to bearings by making a trench on the external part of the outer ring and fixed using a silver lacquer which then was reinforced by a cyanoacrylate glue (fig. 5b).

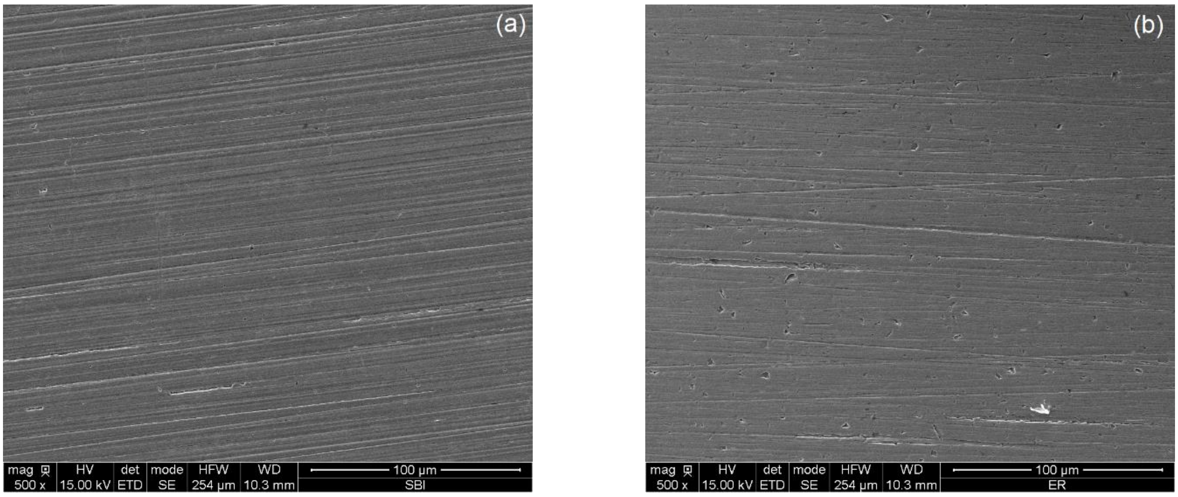

Fig. 2: SEM photography of (a) the inner ring surface and of (b) the roller

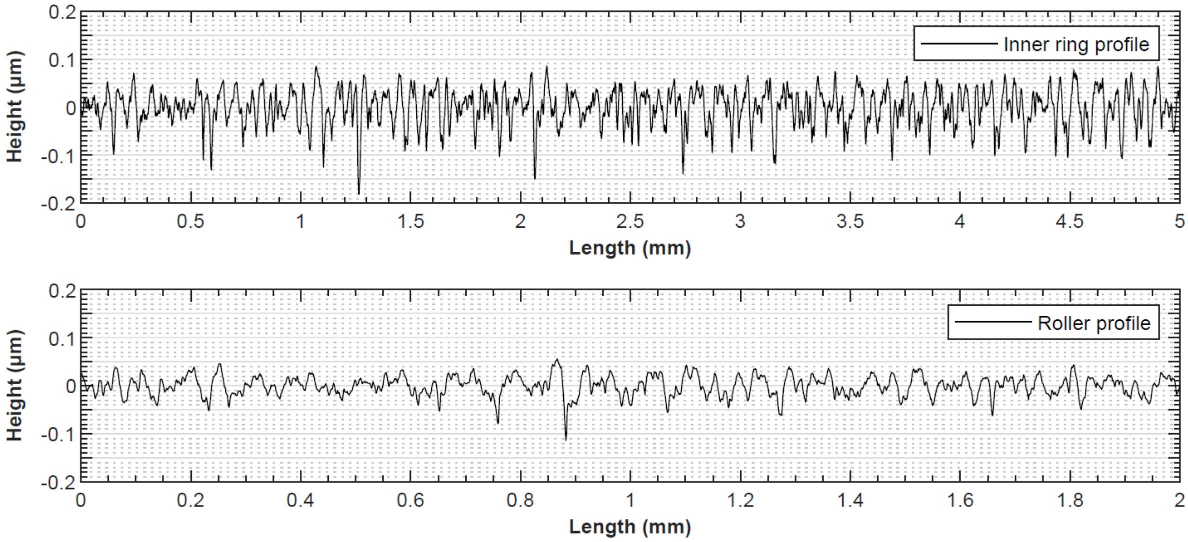

Fig. 3: Roughness profile of contacting surfaces

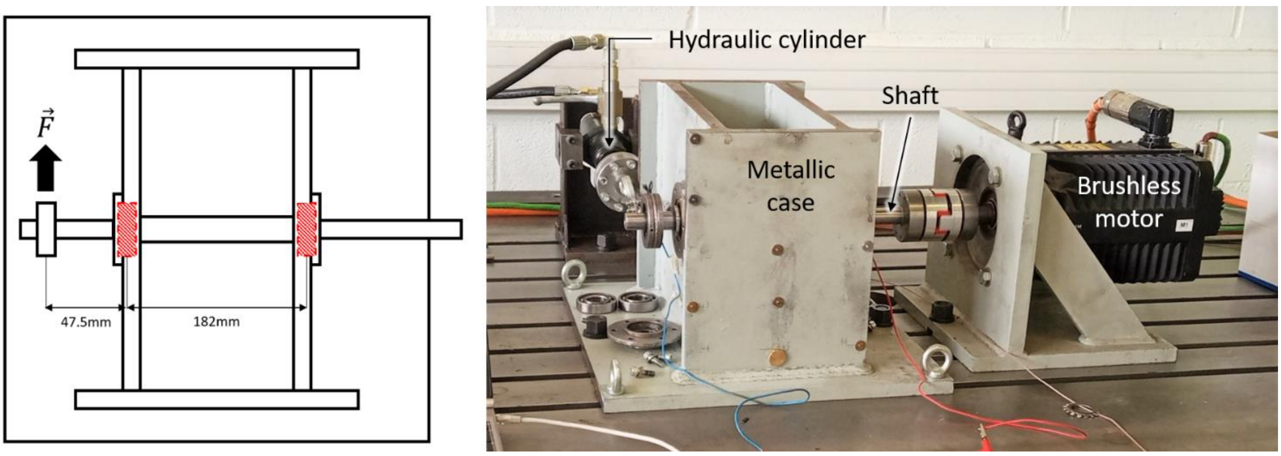

Fig. 4: Experimental bench

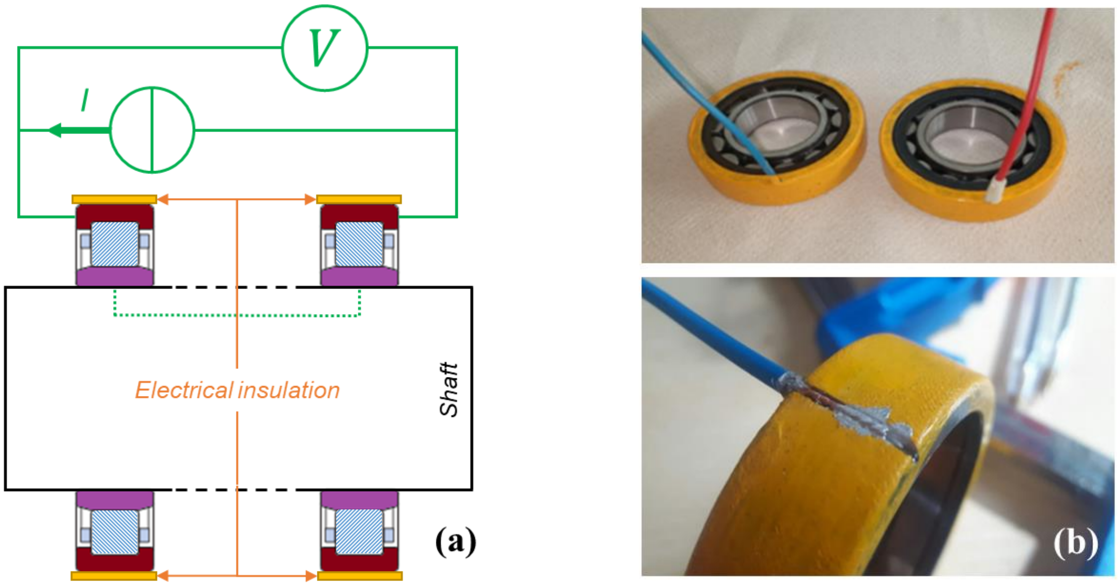

Fig. 5: (a) Electrical measurement method, (b) Fixing the wires

Vibratory measurements were made using a piezoelectric sensor (DJB A/120 VT) with a sensitivity of 1 mV/(m.s^{-2}) - $\pm$ 10%. Furthermore, the data were acquired with an OROS OR36 system. The sensor was placed in the direction of the applied load and fixed with a cyanoacrylate glue (fig. 6).

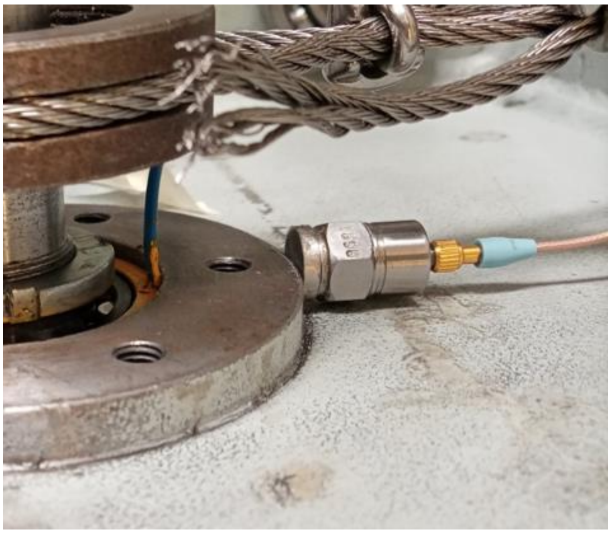

Fig. 6: Position of the vibrations sensor

2.3 Protocol

Once the wires were glued and the insulating paint applied, each component of bearings is reassembled after being cleaned with commercial grade acetone then with alcohol and finally air dried. The cleaning ensure a dry contact between contacting elements. A study in the presence of a third body will be made later, the aim is here to have a reference situation from the electrical point of view. Bearings are then mounted in their respective places and measurement devices set-on.

Electrical and vibratory measurements are made simultaneously during rotation for each value of load and speed. The rotation speed takes the following values [20, 50, 100, 200, 500, 1000] rpm, and the load takes the following values [100, 200, 300] daN. The probing current is fixed to 200 mA, considering that this value does not induce any degradation of the race surface [17]. Each measurement is recorded in a window of 10 seconds with a sample rate of 10 Hz for the electrical method and a sample rate of 25.6 kHz for the vibratory one.

3. RESULTS

3.1 Vibratory analysis

Figure 7 shows a typical vibrations signal accompanied with its spectrum, at 100 rpm and under 300 daN. Sporadic peaks seem to appear in the signal, however nothing relevant emerges from the vibration spectrum: the bearing being new no defect frequency appears (Table 2). The signature of the rotation can be guessed but it is only from 500 rpm that it really appears and is accompanied with few harmonics. That signature is clearer at 1000 rpm: the amplitude at the rotation frequency (16.67 Hz) is even accompanied with seven distinct harmonics.

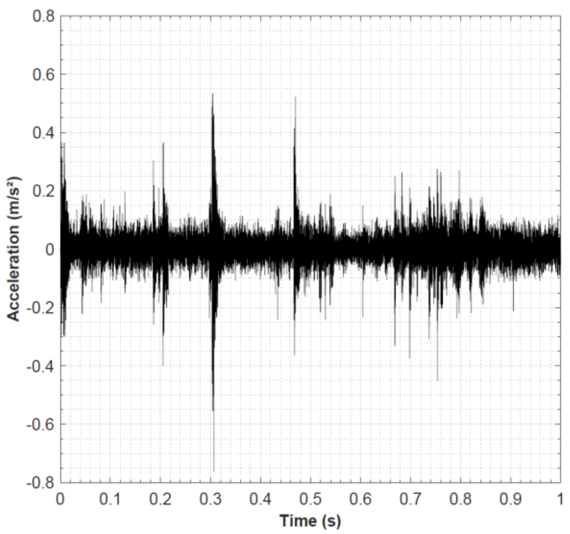

(a)

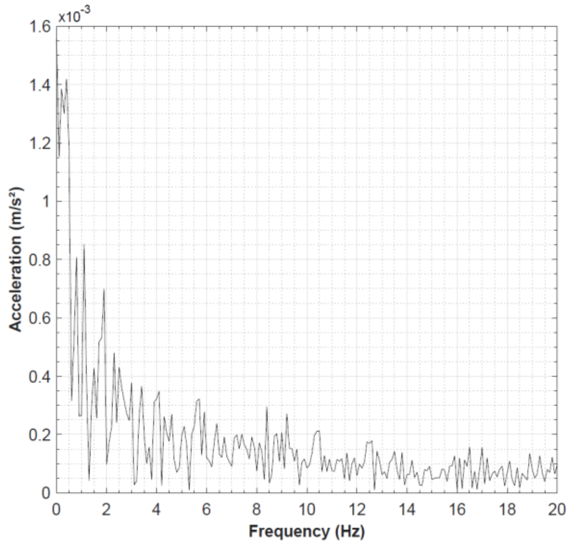

(b)

Fig. 7: (a) Typical vibrations measurement and (b) its spectrum - applied load: 300 daN, rotation speed: 100 rpm

The statistical properties of vibrations, standard deviation, skewness and kurtosis (Table 3) are shown respectively on figure 8a, 8b and 8c. The skewness and the kurtosis exhibit similar behaviors and take high values at low speed: the system seems “unstable” before 200 rpm and then rapidly converge to usual values of a healthy case (0 for the skewness, 3 for the kurtosis). The standard deviation seems to strictly evolve following a power law of the rotation speed ($\sigma_{acc.} = A\omega^{\alpha}$). For each of those parameters, nothing seems to allow to distinguish the effect of the load on the system.

Ordinal	Name	Formula
1	Mean	$\mu = E[x] = \frac{1}{N}\sum_{i=1}^{N} x_i$
2	Variance	$\sigma^2 = E[(x-\mu)^2]$
3	Skewness	$Sk = E\left[\left(\frac{x-\mu}{\sigma}\right)^3\right]$
4	Kurtosis	$Ku = E\left[\left(\frac{x-\mu}{\sigma}\right)^4\right]$

Table 2: Moments calculation

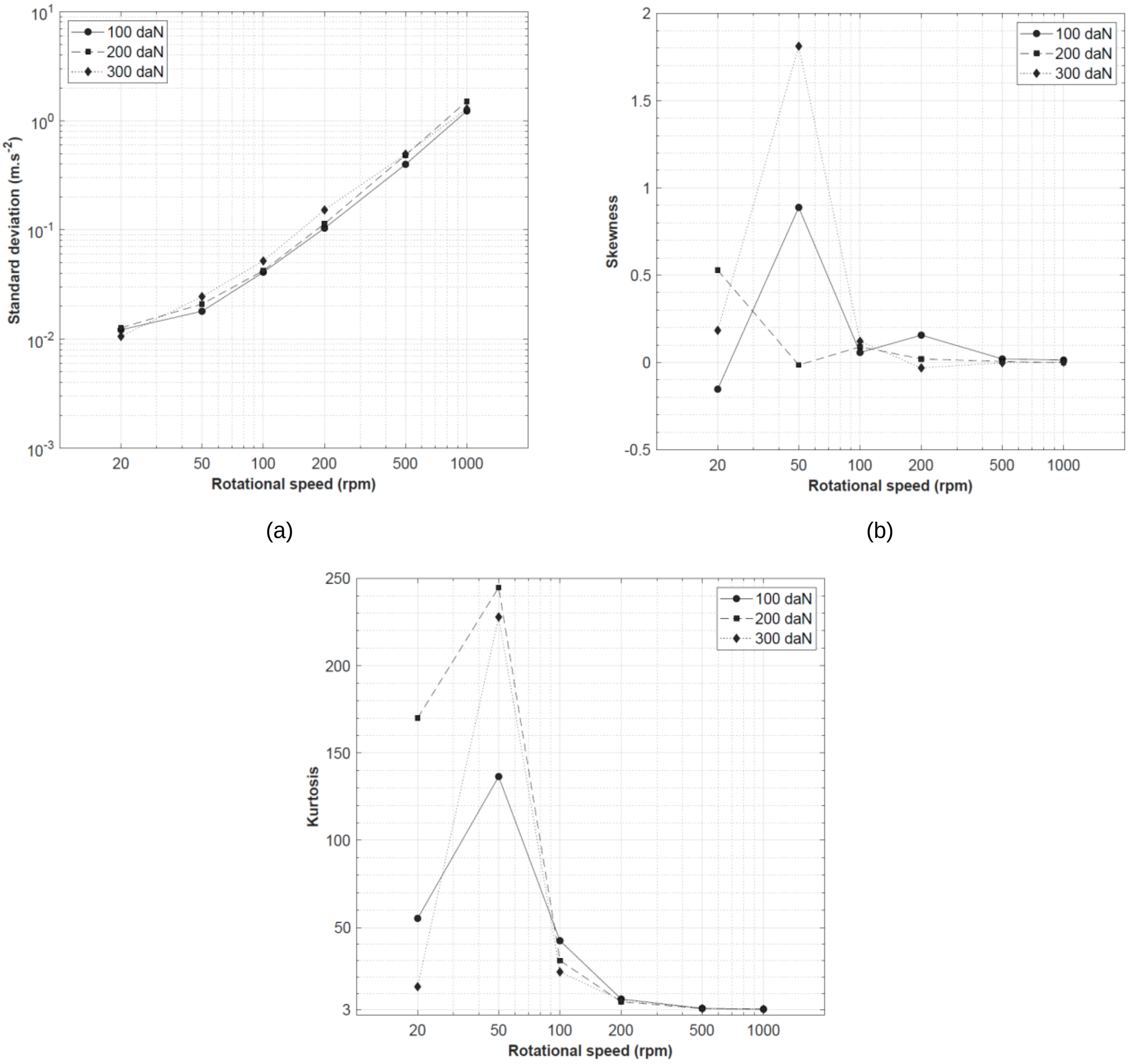

(c)

Fig. 8: (a) Standard deviation, (b) Skewness and (c) Kurtosis of vibrations according to rotation speed and loads

3.2 Electrical analysis

Figure 9 shows typical electrical signal accompanied with its spectrum, at 100 rpm and under 300 daN. The represented signal is obtained from the ratio between the measured voltage V and the imposed current I. Since the current is a constant, the measurement of the voltage is a measurement of the global impedance Z of the system "bearing-shaft-bearing" (fig. 5a). The electrical signal shows oscillations with an unexpected frequency, usually associated to an outer ring defect (BPFO). This signature comes back systemically for each measurements from 100 rpm. Several harmonics of this signature can also be observed.

Figure 10 show the evolution of the amplitude of this signature according to the rotation speed and loads. Overall, the amplitude seems to decrease with the rotation speed and does not seem to be influenced by the applied load. Note that the signature of rotation frequency remains absent in each measurement spectra.

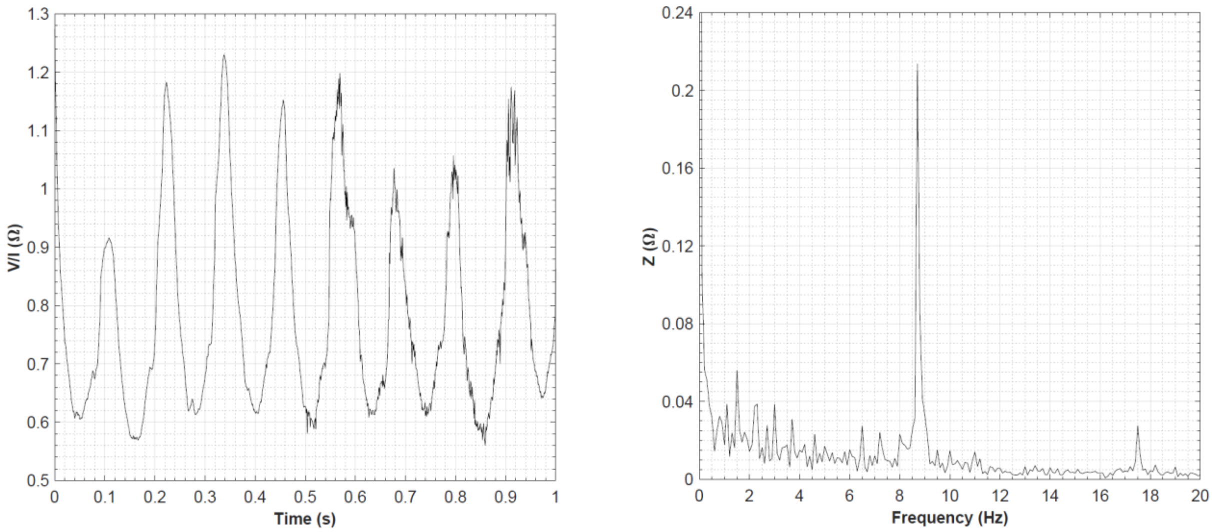

(a) (b)

Fig. 9: (a) Typical electrical measurement and (b) its spectrum - applied load: 300 daN, rotation speed: 100 rpm

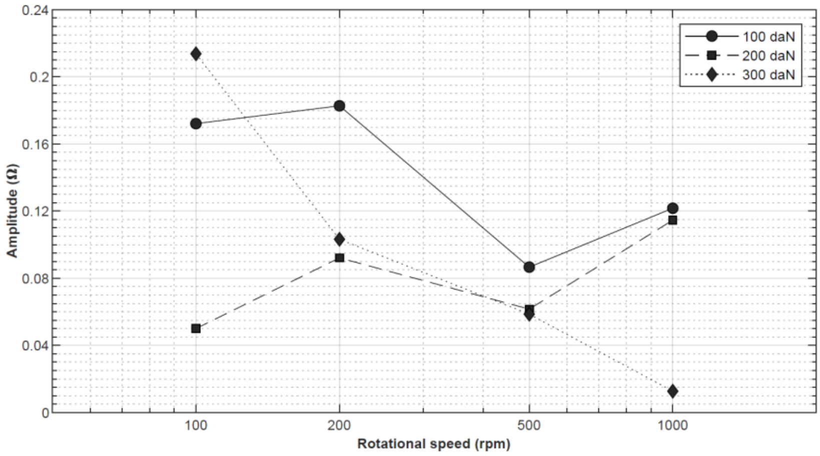

Fig. 10: Evolution of the amplitude of the peak at the load distribution frequency according to the rotation speed

Figure 11 shows the evolution of the mean value of the ratio V/I. As expected, the load has a clearly influence on the system: the contact between each rolling element being better, the electrical resistance from the contact interfaces decreases. The impedance of the system decreases with the rotation speed from 50 to 500 rpm and then seems to increase. The error bars associated to each point are the standard deviation computed from five measurement repetitions.

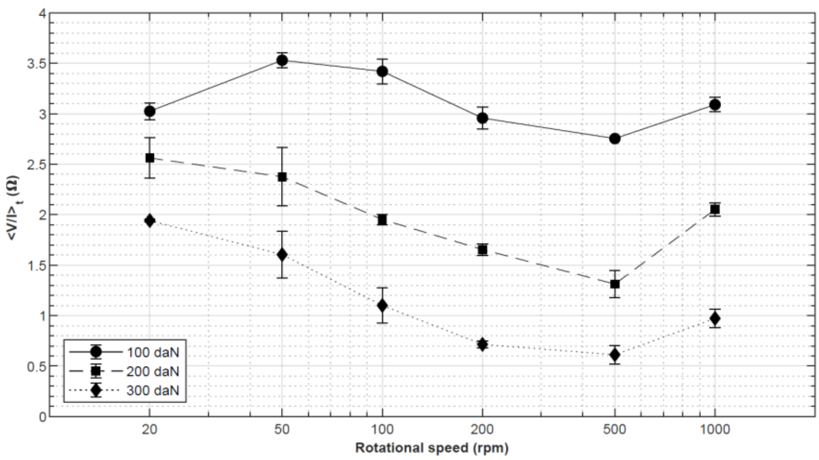

Fig. 11: Evolution of the mean value of the impedance according to the rotation speed

4. DISCUSSION

The unexpected presence of a defect signature in the electric measurements, which is absent in the vibrational ones, needs to be interpreted. Since the bearings are new it is very unlikely that a mechanical defect be present. Nothing in the vibrational analysis seems to contradict this hypothesis: at high speed, the statistical parameters converges to highlight the healthy state of bearings. Two possibilities remains:

(i) The signature is due to an electrical defect, i.e. the conductivity of the outer ring race is not homogeneous. Since bearings are cleaned before measurements, it is possible that during this process the surface chemical properties be altered leading to an inhomogeneity of the conductivity for each element. However, only the signature of BPFO appears: this alteration should lead to the signature of BPFI and BSF (Table 3). Note that this BPFO signature is also detected in ball bearings that don't even undergone any treatment.

Rotation speed (rpm)	Rotation frequency (Hz)	Defect frequencies (Hz)			
		FTF	BSF	BPFO	BPFI
20	0.33	0.134	1.658	1.747	2.586
50	0.83	0.336	4.144	4.368	6.465
100	1.67	0.672	8.289	8.737	12.930
200	3.33	1.344	16.577	17.473	25.860
500	8.33	3.360	41.443	43.683	64.651
1000	16.67	6.720	82.885	87.366	129.301

Table 3: Usual defect frequencies (FTF: Fundamental Train Frequency, BSF: Ball Spin Frequency, BPFO: Ball Passing Frequency of Outer race, BPFI: Ball Passing Frequency of Inner race)

(ii) The signature is due to the modulation of the load distribution inside the bearings. As shown on the figure 12, the load is distributed on the rollers. During the rotation the position of the rollers changes leading to redistribute the load according to the new position of rollers. In a first approximation, assuming that all contacts follow the same behavior, nothing can distinguish the situation a and a'. This phenomenon is obviously periodic and has the same frequency than a BPFO. However, this phenomenon is completely absent from previous works [15, 16], therefore this hypothesis remains uncertain.

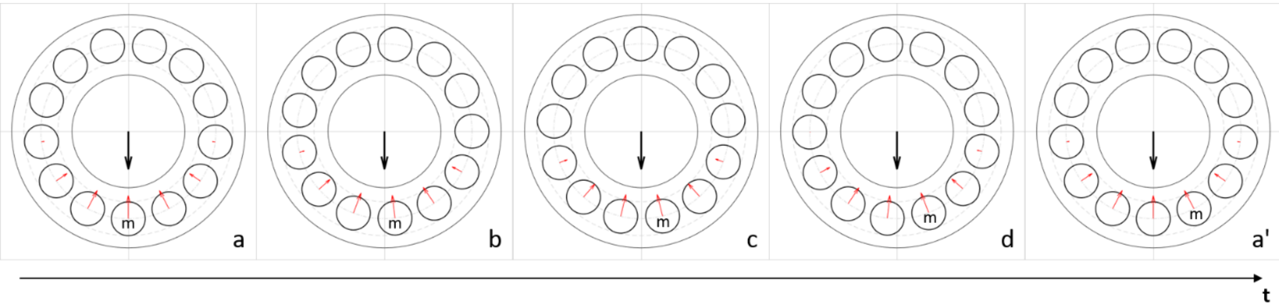

Fig. 12: Load distribution in a roller bearing during rotation

The second hypothesis, if it is true, leads to a problem. If the load distribution frequency and the BPFO are the same, how to distinguish them in the spectrum of signals? This point insists on the need to have a data analysis method which can make the distinction between these two signatures.

Figure 13 shows a comparison of the DC component of the power spectral density (PSD) of each signals between both methods. This last figure shows the relevance of the electrical method: the DC component of electrical signals is clearly influenced by the load and by the rotation speed while that of the vibrations is monotone and load independent. Those results alone sums up all the interest brought by electrical measurement: in this range of forces and speeds, electrical probing provides reliable elements allowing to estimate the operative parameters of the system.

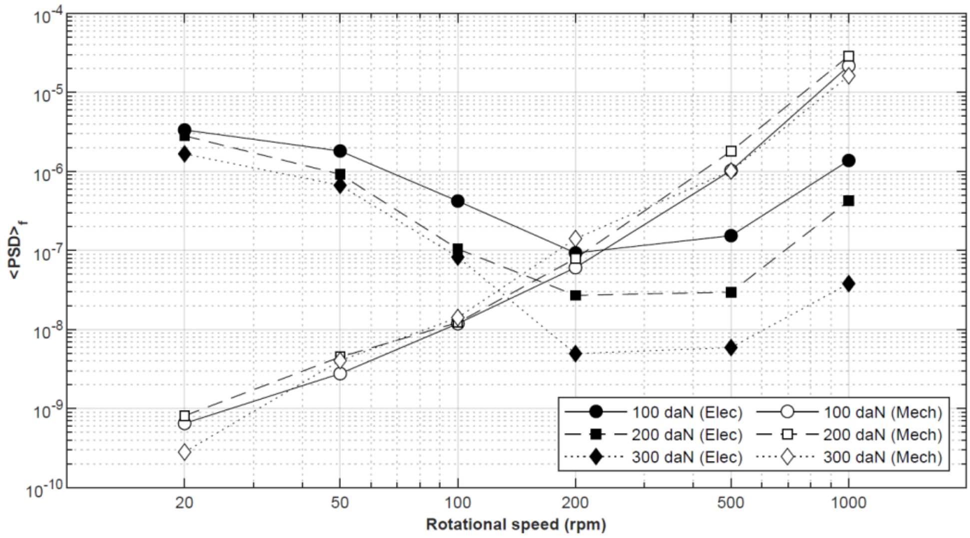

Fig. 13: Evolution of the DC component of the power spectral density according to the rotation speed and load (electrical data are in V^2/Hz and vibrational data in $m^2/s^4/Hz$)

5. CONCLUSION

Support by previous work [14-17], including a patent [19], this work demonstrates the relevance of electrical probing in order to monitor mechanical components such as bearings. This study shows the possibility to access easily - due to its high sensitivity - to operative parameters that a classical method based on vibrations is not able to do. Moreover, electrical probing opens ways to access to the load distribution through a specific signature that could be related to stresses inside the component, which are one of the most important parameters to complete and making more reliable current ageing models.

This study also opens perspectives to research and to compare defect signatures from different methods in order to know the possibility that can offer electrical probing in the monitoring of mechanical components.

ACKNOWLEDGMENTS

The authors thank the University of Reims Champagne-Ardenne for its contribution to the funding of this work. The authors thank also the “Hub de l’énergie” for allowing the use of their surface characterization machines.

REFERENCES

[1] O'Donnell, P. Report of large motor reliability survey of industrial and commercial installations – part 1. IEEE Transactions on Industry Applications, Vol. 21, No. 4, pp 719-864 (1985).

[2] Nandi, S., Toliyat, H.A., and Li, X. Condition monitoring and fault diagnosis of electrical motors – a review. IEEE Transactions on Energy Conversion, Vol. 20, No. 4, pp 719-729 (2005).

[3] Thorsen, O.V., and Dalva, M. Failure identification and analysis for high-voltage induction motors in the petrochemical industry. IEEE Transactions on Industry Applications, Vol. 35, No. 4, pp 810-818 (1999).

[4] Karabay, S., and Uzman, I. Importance of early detection of maintenance problems in rotating machines in management of plants: case studies from wire and tyre plants. Engineering Failure Analysis, Vol.16, No. 1, pp 212-224 (2009).

[5] Randall, R.B., and Antoni, J. Rolling element bearing diagnostics - A tutorial. Mechanical Systems and. Signal Processing, Vol. 25, No. 2, pp 485–520 (2011).

[6] Jian Chen, J., and Randall, R.B. Intelligent diagnosis of bearing knock faults in internal combustion engines using vibration simulation. Mechanism and Machine Theory, Vol. 104, pp 161-176 (2016).

[7] Kerroumi, S., Rasolofondraibe, L., and Chiementin, X. Dynamic Classification: A Tool for Fault Detection and Vibration Behavior Monitoring of Bearings. Proceedings of the ASME 2013, International Mechanical Engineering Congress and Exposition, Vol. 14: Vibration, Acoustics and Wave Propagation. San Diego, California, USA. November 2013.

[8] Ait Sghir, K., Bolaers, F., Cousinard, O., and Dron, J.P. Vibratory monitoring of a spalling bearing defect in variable speed regime. Mechanics & Industry, Vol. 14, No. 2, pp 129-136 (2013).

[9] Kilundu, B., Chiementin, X., Duez, J., and Mba, D. Cyclostationarity of Acoustic Emissions for monitoring bearing defects. Mechanical Systems and Signal Processing, Vol. 25, No. 6, pp 2061-2072 (2011)

[10] Glowacz, A., Glowacz, W., Glowacz, Z, and Kozik, J. Early fault diagnosis of bearing and stator faults of the single-phase induction motor using acoustic signals. Measurement, Vol. 113, pp 1-9 (2018).

[11] Kompella, K.D., Rao, M.V.G., and Rao, R.S. Bearing fault detection in a 3 phase induction motor using stator current frequency spectral subtraction with various wavelet decomposition techniques. Ain Shams Engineering Journal, Vol. 9, No. 4, pp 2427-2439 (2018).

[12] Singh, S. and Kumar, N. Detection of Bearing Faults in Mechanical Systems Using Stator Current Monitoring. IEEE Transactions on Industrial Informatics, Vol. 13, No. 3, pp 1341-1349 (2017).

[13] Jorge Da Silva, J., and De Farias Maribondo, J. Analysis of lubricating oils in shear friction tests using infrared thermography. Infrared Physics and Technology, Vol. 89, pp 291-298 (2018).

[14] Bouzerar, R., Bourny, V., Capitaine, T., and Senlis, J. Characterization of the electrodynamic properties of a ceramic-based ball bearing by impedance spectroscopy. Computer Field Models of Electromagnetic Devices, IOS Press, pp. 842-850 (2010).

[15] Bourbatache, K., Guessasma, M., Bellenger, E., Bourny, V., and Fortin, J. DEM ball bearing model and defect diagnosis by electrical measurement. Mechanical Systems and Signal Processing, Vol. 41, No. 1-2, pp 98-112 (2013).

[16] Machado, C., Guessasma, M., Bellenger, E., Bourbatache, K., Bourny, V., and Fortin, J. Diagnosis of faults in the bearings by electrical measures and numerical simulations. Mechanics & Industry, Vol.15, No. 5, pp 383-391 (2014).

[17] Chevallier, E., Bourny, V., Bouzerar, B., Fortin, J., Durand-Drouhin, O., and Da Ros, V. Voltage noise across a metal/metal sliding contact as a probe of the surface state. Journal of Applied Physics, Vol. 115, pp 1–10 (2014).

[18] Bourny, V., Fortin, J., Capitaine, T., Lorthois, A., and Da Ros V. U.S. Patent No. 9,917,664. Washington, DC: U.S. Patent and Trademark Office (03/13/2018).

[19] Bourny, V., Bouzerar, R., Capitaine, T., Fortin, J., and Lorthois, A. FR Patent No. 3,016,041. Paris, France: Institut National de la Propriété Industrielle (12/30/2013).